Clays and Clay Minerals, Vol. 34, No. 4, 368–378, 1986.

CHEMISTRY OF ILLITE/SMECTITE AND END-MEMBER ILLITE

JAN ŚRODOŃ[1]
Institute of Geological Sciences, Polish Academy of Sciences
31-002 Krakow, Senacka 3, Poland

DAVID J. MORGAN
British Geological Survey, 64 Gray's Inn Road, London WC1X 8NG, United Kingdom

ERIC V. ESLINGER
Cities Service Oil and Gas Corporation, P.O. Box 3908
Tulsa, Oklahoma 74102

DENNIS D. EBERL AND MICHAEL R. KARLINGER
U.S. Geological Survey, MS 404, Federal Center
Denver, Colorado 80225

Abstract—Chemical data from three different series of diagenetic illite/smectites (I/S), analyzed statistically by two regresion techniques, indicate that the content of fixed-K per illite layer is not constant, but ranges from ~0.55 per $O_{10}(OH)_2$ for illite layers in randomly interstratified I/S (R=0; >50% smectite layers) to ~1.0 per $O_{10}(OH)_2$ for illite layers formed in ordered I/S (R>0; <50% smectite layers). By extrapolation of the experimental data, the following chemical characteristics were obtained for end-member illite derived from the alteration of smectite in bentonite: average fixed-K per illite layer = 0.75 per $O_{10}(OH)_2$; total charge = about −0.8; cation-exchange capacity = 15 meq/100 g; surface area (EGME) = 150 m^2/g.

Key Words—Bentonite, Chemical composition, Diagenesis, Illite, Illite/smectite, Smectite.

INTRODUCTION

Illite is a micaceous clay mineral that is a principal constituent of many argillaceous sediments (Grim *et al.*, 1937). Illite derived from the alteration of smectite is considered to be the nonexpanding end-member of the illite/smectite (I/S) series of mixed-layer clays (Hower and Mowatt, 1966). The composition of illite is difficult to determine precisely because illite samples, including the original Fithian illite described by Grim *et al.* (1937), usually are physical mixtures of nonexpanding 10-Å material (i.e., discrete illite) and predominantly illitic, ordered mixed-layer I/S (Środoń, 1984). The present paper attempts to determine the K content of illite layers in I/S and to characterize end-member illite with respect to K content, layer charge, cation-exchange capacity (CEC), and surface area by extrapolating these properties to pure illite from a series of mixed-layer I/S having a broad range of expandabilities and no discrete 10-Å phases.

The first attempt at such an extrapolation was made by Hower and Mowatt (1966) who plotted expandability (percentage of smectite layers) against fixed interlayer-cation content to determine the K content of illite. This plot gave a straight line that extrapolated to ~0.75 fixed K per $O_{10}(OH)_2$ at 0% expandability. This K value is similar to the 0.84 K per $O_{10}(OH)_2$ determined by Weaver (1965) for the illite end-member; both values are significantly smaller than that of muscovite, which ideally has 1.0 K per $O_{10}(OH)_2$.

Hower and Mowatt (1966) did not analyze very expandable clays (i.e., >60% smectite layers), and their plot extrapolates to about 80% expandability for zero fixed cations rather than to 100% expandability as it should if the data were more comprehensive and if the quantity of fixed cations per illite layer was constant throughout the range of expandabilities. This inconsistency inspired the present authors to repeat Hower and Mowatt's plot, using a more complete set of I/S clays and a more accurate method for measuring expandabilities.

MATERIALS AND METHODS

Samples

The samples are from three different geologic ages and geographic locations. Ten samples are Silurian bentonites from the Welsh Borderlands, United Kingdom (Table 1) that occur mainly in shallow-water sequences containing prominent limestone beds. Seventeen samples are Cretaceous bentonites from the

[1] Visiting exchange scientist at the Water Resources Division, U.S. Geological Survey, Denver, Colorado.

Table 1. Chemical analyses of Silurian illite/smectites from the United Kingdom.[1]

Sample[2]	M1	M2	M3	M4	M5	M7	M8	M9	M10	M11
SiO_2	53.28	51.02	52.28	52.10	51.87	50.93	51.25	52.24	49.03	52.58
Al_2O_3	23.06	25.22	19.63	22.69	22.78	24.50	23.53	22.01	23.95	27.04
Fe_2O_3	1.51	1.05	2.14	0.89	1.75	3.07	2.02	1.47	1.94	0.72
FeO	0.28	0.14	0.13	0.28	0.25	0.29	0.33	0.59	0.27	0.24
MgO	3.52	2.58	3.20	3.84	3.35	2.87	3.32	3.80	2.94	2.75
CaO	0.79	1.35	2.24	0.65	1.00	0.99	0.59	1.06	0.94	0.24
Na_2O	0.05	0.05	0.08	0.09	0.05	0.04	0.05	0.34	0.04	0.05
K_2O	6.26	5.48	2.35	6.24	5.98	6.55	7.61	4.97	5.33	8.47
H_2O+	5.92	6.51	6.38	7.34	6.45	6.09	5.87	6.30	6.85	6.61
H_2O-	5.02	6.56	11.45	6.10	6.84	5.52	5.26	7.08	8.34	2.03
TiO_2	0.43	0.23	0.17	0.39	0.14	0.23	0.17	0.35	0.22	0.33
P_2O_5	0.03	0.02	0.02	0.03	0.03	0.03	0.02	0.03	0.02	0.02
Total	100.15	100.21	100.07	100.64	100.49	101.11	100.02	100.24	99.87	101.03

[1] Analysts = M. Joseph, S. F. Hobbs, L. Ault, F. Bin.

[2] M1 = Upper Bringewood Beds (Ludlow), Llangibi, Gwent; M2, M3 = Woolhope Limestone, Overbury, Herefordshire; M4 = Wenlock Limestone, Penny Hill, Worcestershire; M5 = Aymestry Limestone, Woodbury, Worcestershire; M7 = Wenlock Limestone, Wallhouse Plantation, Worcestershire; M8 = Aymestry Limestone, Shavers End, Worcestershire; M9 = Wenlock Limestone, 44-m depth, Manor Farm BH, Rushall, Staffordshire; M10 = Wenlock Limestone, Gleedon Hill, Shropshire; M11 = Wenlock Pentre Beirdd, Powys.

Montana disturbed belt and were described by Eslinger *et al.* (1979). Twenty samples are Upper Carboniferous bentonites from a coal-bearing formation in Upper Silesia, Poland (Table 2). In contrast to the other samples, these last clays are from closely spaced profiles in a single, thick bentonite bed, in which expandabilities have been shown to decrease from the center of the bed to the edges (Środoń, 1976). Three samples are from another Upper Carboniferous bentonite bed from Upper Silesia (Table 2, Brz6, T13, T9). Similar variations in expandability across the bed were noted (Parachoniak and Środoń, 1973).

Sample separation and chemical analysis

The Silurian samples are <5-μm fractions separated from samples in a hydrocyclone. They were analyzed chemically by inductively coupled plasma, atomic-emission spectroscopy (ICP), except for FeO (dichromate titration), P_2O_5 (solution absorptiometry) and H_2O+ and H_2O- (gravimetric). Chemical analyses are given in Table 1.

The Cretaceous samples are <0.1-μm fraction separated from bulk samples by using sodium acetate buffer, 2% Na_2CO_3 treatment, and centrifugation, accord-

Table 2. Chemical analyses of Carboniferous illite/smectites from Upper Silesia, Poland. X-ray fluorescence analyses (recalculated to 100 wt. % of ignited material).

Sample	2M9	2M5	2M3	4M2	1Cz212	2R50	1Cz213	2R49	1M6	Ch5	2R63	2R62
SiO_2	65.79	63.47	63.83	64.74	63.26	63.50	63.94	61.44	62.33	61.14	60.35	61.47
TiO_2	0.08	0.81	0.09	0.09	0.08	0.23	0.06	0.22	0.12	0.06	0.23	0.18
Al_2O_3	22.53	22.56	23.84	22.84	24.46	22.45	23.48	24.35	24.94	26.39	24.67	24.95
Fe_2O_3	3.18	3.54	3.25	3.62	3.30	4.00	3.21	3.64	2.87	2.64	3.48	3.07
MgO	3.38	3.89	3.75	3.44	3.61	3.71	3.81	3.57	3.59	3.22	3.78	4.08
CaO	0.18	0.29	0.15	0.17	0.18	0.18	0.15	0.21	0.15	0.17	0.18	0.24
Na_2O	0.03	0.11	0.06	0.08	0.06	0.32	0.09	0.06	0.09	0.10	0.06	0.16
K_2O	0.94	0.96	1.49	1.79	2.15	2.36	2.69	3.74	4.57	5.43	5.27	5.22
SrO	4.38	4.36	4.10	3.91	3.70	3.25	3.44	2.77	2.55	2.41	1.97	2.07

Direct-current, plasma-emission spectroscopy analyses (averages of two analyses per sample).

Sample	Brz6	R83	R81	R86	R85	R84	R80	R78	3M2	T13	T9
SiO_2	52.9	53.1	53.5	56.0	56.9	55.3	53.3	53.0	54.8	49.7	51.6
TiO_2	0.196	0.049	0.052	0.080	0.083	0.050	0.066	0.056	0.075	0.052	0.191
Al_2O_3	18.9	19.2	19.1	20.4	20.3	19.6	20.2	20.1	20.7	23.0	23.6
Fe_2O_3	1.12	3.34	3.58	2.44	2.52	3.13	2.72	2.37	2.89	1.26	3.57
MgO	3.52	3.04	3.03	3.18	3.03	3.23	2.64	3.00	2.92	2.29	2.06
MnO	0.003	0.016	0.006	0.007	0.016	0.021	0.003	0.003	0.008	0.002	0.008
CaO	0.268	0.686	0.481	0.266	0.718	0.469	0.348	0.496	0.910	0.336	0.109
Na_2O	2.08	1.49	1.76	1.95	1.29	1.94	1.12	0.507	1.61	1.96	0.915
K_2O	1.66	1.51	1.62	2.34	2.24	1.82	2.50	2.88	3.61	4.78	6.24

https://doi.org/10.1346/CCMN.1986.0340403 Published online by Cambridge University Press

Table 3. Structural formulae, cation-exchange capacity, surface area, and mineralogical characteristics of Silurian illite/smectites from the United Kingdom.

Sample	M11	M8	M7	M4	M1	M5	M2	M10	M9	M3
Tetrahedral										
Si	3.53	3.59	3.54	3.67	3.68	3.66	3.62	3.56	3.69	3.77
Al	0.47	0.41	0.46	0.33	0.32	0.34	0.38	0.44	0.31	0.23
Octahedral										
Al	1.68	1.54	1.55	1.56	1.56	1.55	1.62	1.60	1.52	1.52
Fe^{3+}	0.03	0.09	0.15	0.04	0.06	0.09	0.06	0.10	0.07	0.11
Fe^{2+}	0.01	0.02	0.01	0.01	0.01	0.01	0.01	0.01	0.03	0.01
Mg	0.28	0.35	0.30	0.40	0.37	0.35	0.30	0.32	0.40	0.38
Sum	2.00	2.00	2.01	2.01	2.00	2.00	1.99	2.03	2.02	2.02
Charge	−0.29	−0.37	−0.28	−0.38	−0.38	−0.36	−0.34	−0.24	−0.37	−0.33
Total layer charge	−0.76	−0.78	−0.74	−0.71	−0.70	−0.70	−0.72	−0.68	−0.68	−0.56
Fixed-K	0.72	0.67	0.58	0.55	0.55	0.53	0.52	0.49	0.44	0.24
Exchangeable										
Ca	0.01	0.04	0.07	0.06	0.06	0.07	0.09	0.08	0.08	0.15
Na	0.01	0.01	0.01	0.01	0.01	0.00	0.00	0.00	0.04	0.01
K	0.00	0.00	0.00	0.01	0.00	0.01	0.01	0.01	0.02	0.00
Interlayer charge	+0.75	+0.76	+0.73	+0.69	+0.68	+0.68	+0.71	+0.66	+0.66	+0.55
CEC (meq/100 g)	15.3	22.3	27.1	33.9	33.6	37.9	44.0	45.1	47.9	74.8
Surface area (m^2/g)	151	220	247	291	294	327	331	322	405	596
% Smectite layers	6	7	13	15	20	25	29	31	38	66
Type of ordering	R=3	R=3	R=3	R=1/R=3	R=1/R=3	R=1	R=1	R=1	R=0/R=1	R=0

ing to methods described in Eslinger *et al.* (1979). Chemical analyses were made by atomic absorption spectroscopy (AA), and Fe^{2+}/Fe^{3+} ratios were obtained from Mössbauer spectroscopic data. Chemical analyses were reported in Eslinger *et al.* (1979).

Twelve of the Carboniferous samples are <0.125-μm fractions obtained from 1 N NaCl-exchanged bentonites. They were subsequently exchanged with Sr by four washings with 1 N $SrCl_2$, dialyzed, and analyzed chemically by X-ray fluorescence spectrometry (XRF) using a technique described by Hower *et al.* (1964), except that Na was determined by flame photometry (Hoffman and Hower, 1979). The other 11 Carboniferous samples are <0.3-μm fractions that were separated from natural samples by centrifugation and analyzed by direct-current, plasma-emission spectroscopy (DCP). Single samples from the other sets also were analyzed in this manner to compare data obtained by the different analytical techniques. Replicate analyses were made for each of these samples (two dissolutions per sample, Medlin *et al.*, 1969). K_2O was determined by AA. Chemical analyses for the Carboniferous samples are reported in Table 2.

Structural formulae

Structural formulae were calculated by normalizing cation analyses to a theoretical structure containing $O_{10}(OH)_2$. For the Silurian samples, dithionite-extractable Fe^{3+} was determined separately and subtracted from the complete chemical analysis before calculation of the formulae in order to eliminate the effect of iron coatings. Exchangeable K was measured by analysis of NH_4OAc extracts. Ti was not included in the calculation because X-ray powder diffraction (XRD) analysis detected anatase in some of the samples. Semiquantitative XRD analysis also led to the subtraction of 7% kaolinite from the chemical analysis of sample M2, and 3% kaolinite and 4% quartz from the analysis of sample M3, before the formulae were calculated (Table 3).

For the 12 Carboniferous samples analyzed by XRF, Sr and minor quantitites of Ca and Na were assumed to be exchangeable cations, and K was assumed to be nonexchangeable (i.e., fixed in the interlayer of illite layers). All Fe was treated as Fe_2O_3. In addition, 1.5% kaolinite was subtracted from the analysis of sample 2R63. Ti was not included in the formulae (Table 4). For the 11 Carboniferous samples analyzed by DCP, K was assumed to be fixed, and Na and Ca were assumed to be exchangeable. Ti was not included in the calculation, and all Fe was treated as Fe_2O_3 (Table 4). Some samples from this set gave anomalously small values for octahedral occupancy (<1.97), probably due to contamination by NaCl. Recalculation of the formulae, assuming less Na_2O, gave octahedral occupancies of about 2.0. The value for fixed K was not affected by this recalculation, but layer charge values were affected significantly. For this reason, formulae with octahedral occupancies differing from 2.0 by more than ±0.03 were used for fixed-K determinations, but not for layer charge estimates.

For the Cretaceous samples, all K was assumed to

https://doi.org/10.1346/CCMN.1986.0340403 Published online by Cambridge University Press

Table 4. Structural formulae and mineralogical characteristics of Carboniferous illite/smectites from Upper Silesia, Poland.

Sample	2M9	2M5	2M3	4M2	1Cz212	2R50	1Cz213	2R49	1M6	Ch5	2R63	2R62
Tetrahedral												
Si	3.95	3.88	3.85	3.90	3.81	3.87	3.85	3.77	3.77	3.70	3.72	3.72
Al	0.05	0.12	0.15	0.10	0.19	0.13	0.15	0.23	0.23	0.30	0.28	0.28
Octahedral												
Al	1.54	1.50	1.54	1.52	1.55	1.48	1.52	1.53	1.55	1.58	1.49	1.50
Fe	0.14	0.16	0.15	0.17	0.15	0.18	0.15	0.17	0.13	0.12	0.17	0.14
Mg	0.30	0.35	0.34	0.31	0.32	0.34	0.34	0.33	0.32	0.29	0.35	0.37
Sum	1.98	2.01	2.03	2.00	2.02	2.00	2.01	2.03	2.00	1.99	2.01	2.01
Charge	−0.36	−0.32	−0.25	−0.31	−0.26	−0.34	−0.31	−0.24	−0.32	−0.32	−0.32	−0.34
Total layer charge	−0.41	−0.44	−0.40	−0.41	−0.45	−0.47	−0.46	−0.47	−0.55	−0.62	−0.60	−0.62
Fixed-K	0.07	0.07	0.11	0.14	0.17	0.18	0.21	0.29	0.35	0.44	0.41	0.40
Exchangeable												
Ca	0.01	0.02	0.01	0.01	0.01	0.01	0.01	0.01	0.01	0.01	0.01	0.02
Na	0.00	0.01	0.01	0.01	0.01	0.05	0.01	0.01	0.01	0.00	0.01	0.02
Sr	0.15	0.15	0.14	0.14	0.13	0.11	0.12	0.10	0.09	0.10	0.07	0.07
Interlayer charge	+0.39	+0.42	+0.42	+0.45	+0.46	+0.47	+0.48	+0.52	+0.56	+0.66	+0.58	+0.60
% Smectite layers	88	85	81	78	71	62	58	48	41	37	32	29
Type of ordering	R=0	R=0	R=0	R=0	R=0	R=0	R=0	R=0/R=1	R=0/R=1	R=0/R=1	R=1	R=1

Sample	Brz6	R83	R81	R86	R85	R84	R80	R78	3M2	T13	T9
Tetrahedral											
Si	3.88	3.84	3.84	3.85	3.89	3.85	3.83	3.84	3.78	3.62	3.61
Al	0.12	0.16	0.16	0.15	0.11	0.15	0.17	0.16	0.22	0.38	0.39
Octahedral											
Al	1.51	1.47	1.45	1.50	1.52	1.46	1.54	1.56	1.46	1.59	1.55
Fe	0.06	0.18	0.20	0.13	0.13	0.17	0.15	0.13	0.15	0.07	0.19
Mg	0.38	0.33	0.32	0.33	0.31	0.33	0.28	0.32	0.30	0.25	0.21
Sum	1.95	1.98	1.97	1.96	1.96	1.96	1.97	2.01	1.91	1.91	1.95
Charge	−0.53	−0.39	−0.41	−0.45	−0.43	−0.45	−0.37	−0.29	−0.57	−0.52	−0.36
Total layer charge	−0.65	−0.55	−0.57	−0.60	−0.54	−0.60	−0.54	−0.45	−0.79	−0.90	−0.75
Fixed-K	0.16	0.14	0.15	0.20	0.19	0.16	0.23	0.27	0.32	0.44	0.56
Exchangeable											
Ca	0.02	0.05	0.04	0.02	0.05	0.03	0.03	0.04	0.07	0.03	0.01
Na	0.44	0.31	0.36	0.38	0.25	0.39	0.23	0.11	0.32	0.41	0.18
Interlayer charge	+0.64	+0.55	+0.59	+0.62	+0.54	+0.60	+0.52	+0.46	+0.78	+0.91	+0.76
% Smectite layers	66	76	71	69	68	68	61	59	45	37	20
Type of ordering	R=0	R=0	R=0	R=0	R=0	R=0	R=0	R=0	R=0	R=1	R=1/R=3

Table 5. Fixed-K, total layer charge and mineralogical characteristics of Cretaceous illite/smectites from Montana.[1]

Sample	Fixed K[2]	Total layer charge	% smectite layers	Type of ordering
LT-42	0.05	−0.42	98	R=0
LT-139A	0.06	−0.45	97	R=0
LT-1	0.10	−0.46	88	R=0
LT-69C	0.19	−0.50	70	R=0
LT-158	0.22	−0.47	56	R=0
LT-4	0.31	−0.50	46	R=0
LT-128	0.34	−0.52	43	R=1
LT-85	0.38	−0.56	40	R=1
LT-96A	0.40	−0.57	40	R=1
LT-162	0.41	−0.54	33	R=1
LT-51	0.43	−0.58	33	R=1
LT-10B	0.41	−0.55	32	R=1
LT-93A	0.42	−0.58	31	R=1
LT-109	0.45	−0.57	27	R=1
LT-24	0.49	−0.61	26	R=1
LTE-21	0.50	−0.60	20	R=1
LT-21	0.46	−0.59	19	R=1

[1] From Eslinger *et al.* (1979).
[2] Per $O_{10}(OH)_2$.

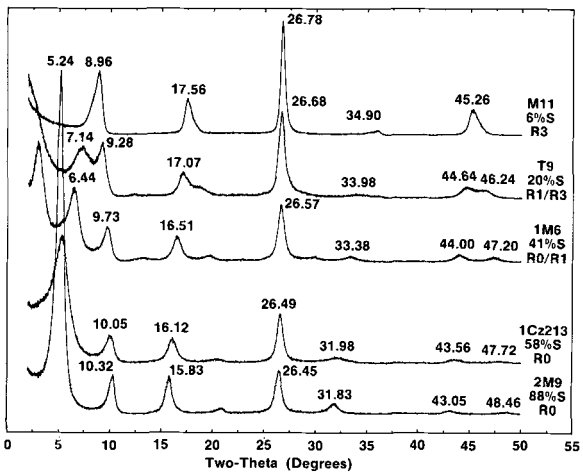

Figure 1. X-ray powder diffraction patterns of I/S encompassing range of expandabilities studied. Patterns are of oriented, ethylene glycol-solvated preparations using CuKα radiation. Peak positions and sample identification are given in the figure. %S = percentage of smectite layers (expandability); R0 = random interstratification; R1, R3 = types of ordered interstratifications.

be fixed because all samples were Na-exchanged during separation. Like some of the Carboniferous samples, most of the Cretaceous samples were assumed to be Na-contaminated; therefore, the structural formulae given by Eslinger *et al.* (1979) were based on an average CEC for a given expandability. This approach gave octahedral occupancies close to 2.0; both total charge and fixed K from these analyses are used in the present paper (Table 5).

Formulae for three samples, each analyzed by two methods, are given in Table 6. Fixed-K values differ by no more than 5%, but layer-charge values differ by as much as 20%. Thus, fixed-K values obtained from different analytical techniques are comparable. Layer-charge values, however, should be analyzed in sets obtained by one analytical technique, and only the trends, and not the absolute values, can be compared between sets.

Cation-exchange capacity and surface area

Cation-exchange capacities (CEC) were obtained only for the Silurian samples. CEC was measured by the

Table 6. Structural formulae of three samples analyzed by different techniques.

	LT-139A		LTE-21		M11	
Technique	AA[1]	DCP[2]	AA[1]	DCP[2]	ICP[3]	DCP[2]
Tetrahedral						
Si	3.61	3.66	3.48	3.52	3.53	3.53
Al	0.39	0.34	0.52	0.48	0.47	0.47
Octahedral						
Al	1.43	1.46	1.71	1.73	1.68	1.67
Fe^{3+}	0.23	0.24	0.08	0.12	0.03	0.05
Fe^{2+}	0.00	—	0.04	—	0.01	—
Mg	0.18	0.17	0.19	0.17	0.28	0.25
Sum	1.84	1.87	2.02	2.02	2.00	1.97
Charge	−0.66	−0.56	−0.17	−0.11	−0.29	−0.34
Total-layer charge	−1.05	−0.90	−0.69	−0.59	−0.76	−0.81
K	0.06	0.06	0.50	0.53	0.72	0.75
Ca	0.06	0.01	0.05	0.00	0.01	0.02
Na	0.85	0.82	0.06	0.06	0.01	0.02
Interlayer charge	+1.03	+0.90	+0.66	+0.59	+0.75	+0.81

[1] Atomic absorption spectroscopy.
[2] Direct-current, plasma-emission spectroscopy.
[3] Inductively coupled plasma, atomic-emission spectroscopy.

https://doi.org/10.1346/CCMN.1986.0340403 Published online by Cambridge University Press

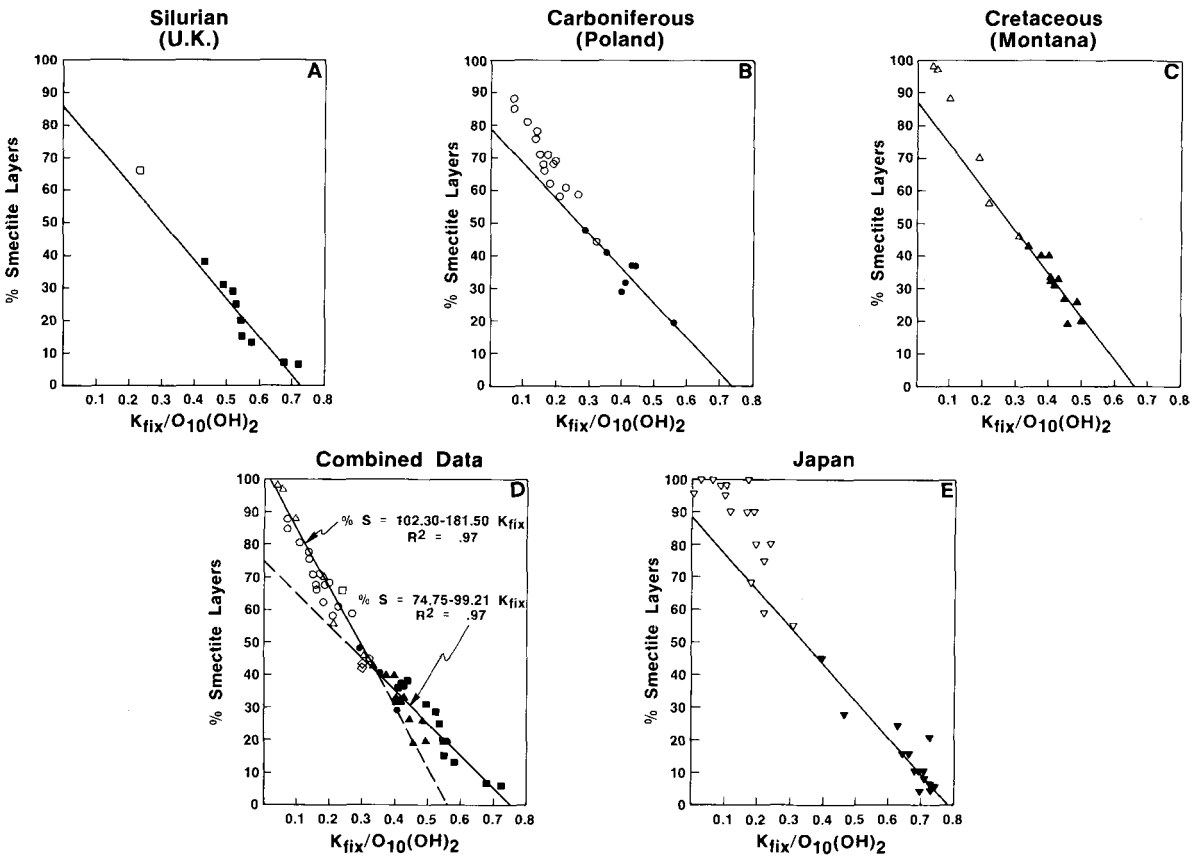

Figure 2. Plots of fixed potassium vs. expandability for I/S. On plots representing individual sets of samples (A–C), the best-fit lines for ordered minerals are drawn to show that random samples plot above them. On plot combining all data (D), lines obtained from regression analysis are drawn both for random and ordered minerals. The two diamonds (◇) are for two Ordovician samples from Kinnekulle, Sweden (authors' data; DCP analyses). Data from Inoue and Utada (1983) are shown in plot E. Open symbols = R0 ordering minerals; solid symbols = partially ordered to completely ordered minerals.

ammonium acetate method of Mackenzie (1951). Surface area was measured by the ethylene glycol-monoethyl ether (EGME) method of Carter *et al.* (1965).

X-Ray powder diffraction identification

The Silurian samples were analyzed by XRD in the Ca-form, the Cretaceous samples in the Na-form, and the Carboniferous material in the natural form (exchange complex dominated by Na). Suspensions of the samples were pipeted onto glass slides (~0.7 mg clay/cm^2), and were solvated with ethylene-glycol using the liquid technique of Środoń (1980). Samples were examined with a Siemens Automated D500 diffraction system using a Cu-tube, a graphite monochromator, a 2θ range of 2°–50°, steps of 0.02°2θ, and a counting time of 4 s/step.

The layer ratio and the type of ordering of I/S were determined as described by Środoń (1980, 1984). Layer ratios of samples containing more than ~20% smectite layers were measured by the Δd_2 technique using reflections in the 40°–50°2θ range (CuKα radiation; Środoń, 1980, Figure 5). Samples that contained less expandable I/S were identified by the method outlined by Środoń (1984). Peak positions were chosen in the middle of the uppermost part of the peak. The precision of all the measurements was ±1–3% smectite layers. Examples of the XRD data are shown in Figure 1. Peak positions, percentage of smectite layers, and type of interstratification are marked on the figure.

RESULTS

Potassium content of illite layers

Several plots of quantity of fixed-K vs. expandability are presented in Figure 2. A plot of original data from Inoue and Utada (1983) is shown also (Figure 2E), because it illustrates what is probably one of the most complete sequences of I/S reported to date.

From these plots the following features were observed: (1) Data that include the complete range of expandabilities cannot be fitted closely by a single straight line, as was attempted by Eslinger *et al.* (1979) and Inoue and Utada (1983). (2) Data for ordered I/S (<50% smectite layers) can be fitted by a straight line

https://doi.org/10.1346/CCMN.1986.0340403 Published online by Cambridge University Press

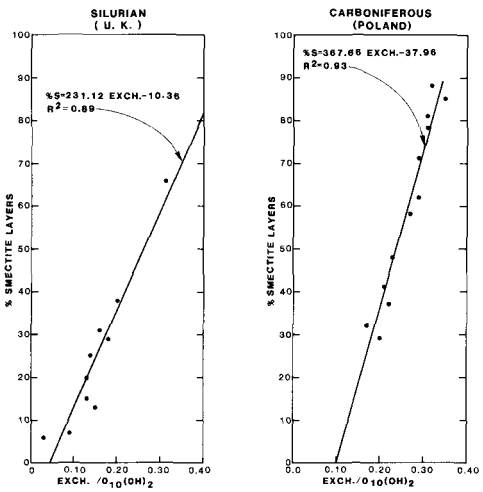

Figure 3. Plots of equivalents of exchangeable cations vs. expandability of I/S for Silurian and the Carboniferous samples. Note different slopes of best-fit lines, reflecting different charges/smectite layer for two different sample sets.

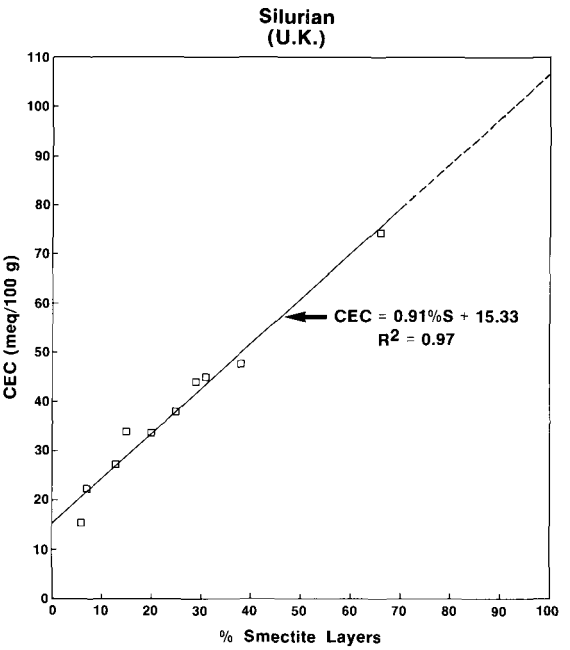

Figure 4. Plot of cation-exchange capacity vs. expandability of I/S for Silurian samples.

extrapolating to ~0.75 fixed-K for pure end-member illite. Like the original plot made by Hower and Mowatt (1966), this line does not extrapolate to 100% smectite layers for zero fixed-K, but rather to about 75% smectite layers. (3) Data for randomly interstratified (R=0) I/S (>50% smectite layers) can be fitted by a straight line that extrapolates to ~0.55 fixed-K for pure end-member illite. This line also does not extrapolate exactly to 100% smectite layers for zero fixed-K, but rather to ~102% smectite layers. If this misfit is not due to a systematic analytical error, it indicates the presence of a small fraction of high-charge illite layers at very high expandabilities. A possible origin for these layers is discussed below. (4) The data of Inoue and Utada (1983) show the same characteristics as those plotted in Figure 2D, although dispersion of the analytical points is greater, probably due to less-precise expandability measurements.

A regression analysis was performed to determine if the relationship between fixed K and percentage of smectite is consistent among populations of interstratified clays for which R=0 and R>0. The percentage of smectite layers was the dependent variable, and fixed-K was the primary independent variable. In addition to fixed-K, indicator variables distinguishing R=0 from R>0 were included in the independent variable set. For example, if Z was an indicator variable, it was assigned a value of 0.0 if the percentage of smectite was from a R>0 clay; Z was assigned a value of 1.0 if the percentage of smectite layers was from R=0 clay. Coefficients of these variables were used to detect significant changes in the proposed regression model resulting from clay-population differentiation. Any change in intercept was determined from the significance and value of the coefficient of the indicator variable Z; change in slope was determined from the properties of the indicator variable Z multiplied by the amount of fixed K. The results indicate that the two clay populations are significantly different (at the >99% level) as they relate to fixed potassium. The resulting two models are:

Random clay: % smectite layers =
102.30 − (181.50)(fixed-K);
Ordered clay: % smectite layers =
74.75 − (99.21)(fixed-K).

The point of intersection of the above regression lines is at a fixed-K value of about 0.33 and a corresponding smectite layer value of 42%. The coefficient of determination (R^2) for these two lines is .97, whereas R^2 is .95 if all of the data were fitted to a single line; hence the two-line fit is somewhat more likely. In addition, a plot of residuals for the single-line model shows non-uniform scatter along the line, indicating that this model is invalid because it violates the assumption of ordinary least squares regression.

A statistical analysis was performed to determine if the relationship between fixed-K and percentage of smectite for a *mixed* population of R=0 and R>0 clays is consistent through the entire range of fixed-K values. Indicator variables were used here also, but the differentiation was based on fixed-K values. Because no *a priori* assumption was made for the exact location of any break in slope for fixed-K, sequential regression analyses were applied; each time a progressively larger value of fixed-K was selected from the data set as the

https://doi.org/10.1346/CCMN.1986.0340403 Published online by Cambridge University Press

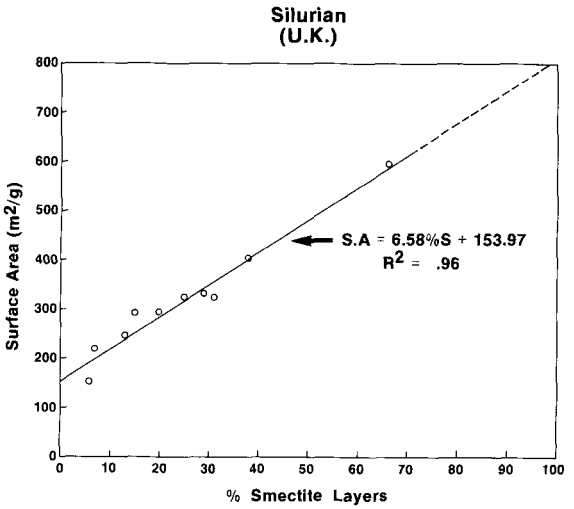

Figure 5. Plot of surface area vs. expandability of I/S for Silurian samples.

assumed breakpoint. If the fixed-K value was less than the assumed breakpoint, an indicator variable Z was assigned a value of 1.0; if the value was greater than or equal to the assumed breakpoint, Z was assigned a value of 0.0. These values of fixed-K ranged from 0.23 to 0.44, which, based on Figure 2, seemed to contain an apparent breakpoint, while assuring sufficient degrees of freedom for the regression technique.

The coefficients of the indicator variables were statistically significant (at the >99% level) for all sequential regressions. The breakpoint was chosen to be that measured value of fixed-K whose corresponding regression accounted for the most statistically significant coefficients of the indicator variables. In addition, because the distribution of data points indicated continuity for the range of values considered, the breakpoint could also be determined as the location at which the combined effect of the indicator variables was zero, relative to the two models. These criteria are similar to those used in more formal spline-fitting analyses.

This analysis indicated that the breakpoint location of fixed-K was ~0.31 and that the two models are as follows:

Fixed-K <0.31: % smectite layers =
103.96 − (194.09)(fixed-K)

Fixed-K ≥0.31: % smectite layers =
76.87 − (103.26)(fixed-K).

The point of intersection of these two models is at ~0.30 fixed-K and a corresponding smectite layer percentage of 46.

Thus, the first type of regression analysis indicates that two populations are present in Figure 2D if the data are divided into R=0 and R>0 clay populations. The second analysis indicates that a break in the regression relation occurs at a K value which closely corresponds to the break between R=0 and R>0 clay populations.

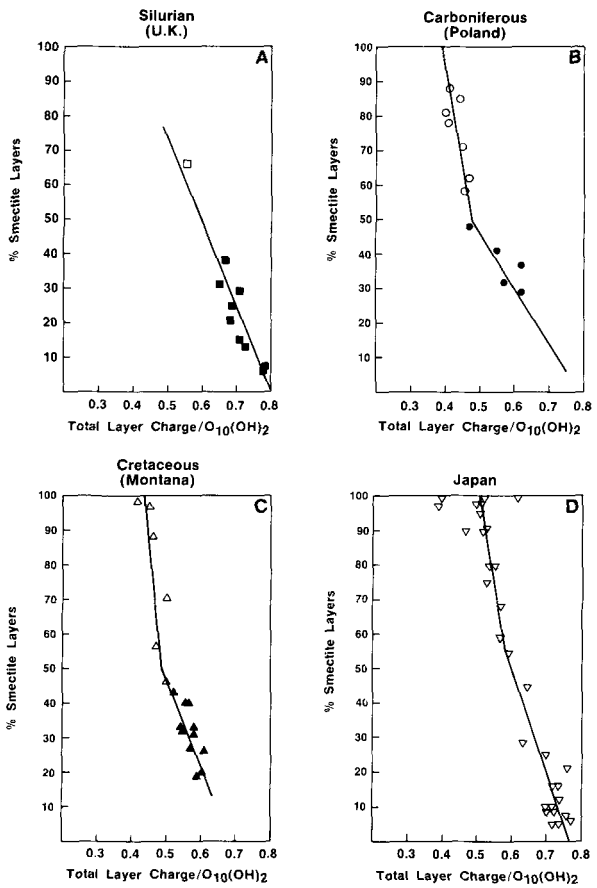

Figure 6. Plots of charge density vs. expandability for I/S. Note break in slopes at ~50% expandable. Data from Inoue and Utada (1983) showing same feature are included (D).

Other chemical characteristics of the illite/smectite series

Plots of the equivalents of exchangeable cations vs. expandability for the Silurian and the Carboniferous sets of samples can be fitted by straight lines with large correlation coefficients (Figure 3). Data from the Carboniferous samples are complete enough to conclude that this relationship is linear throughout the entire expandability range. For pure illite, the lines extrapolate to 0.04–0.1 equivalents of exchangeable cations per one-half unit cell, which is interpreted as the CEC of pure illite.

The slopes of the two lines are different, showing greater charge densities for smectite layers in the Silurian samples. Such higher charge densities are consistent with small thicknesses of smectite-ethylene glycol complexes for the Silurian samples (see, e.g., Środoń, 1984, Figure 4, samples 15(T9) and 16(M1)); smaller thicknesses are indicative of greater charge densities (Środoń, 1980).

https://doi.org/10.1346/CCMN.1986.0340403 Published online by Cambridge University Press

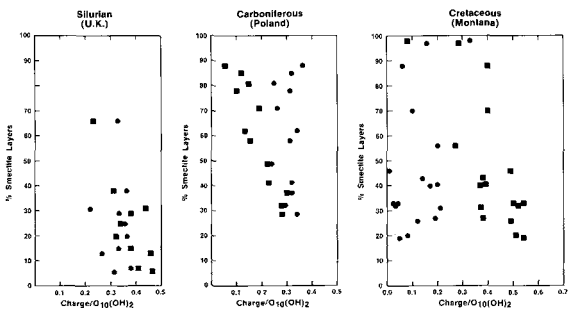

Figure 7. Plots of tetrahedral (■) and octahedral (●) charge vs. expandability for I/S. Note large scatter for data and different values for different sets, but generally stable octahedral charges and tetrahedral charges increasing with decreasing expandability.

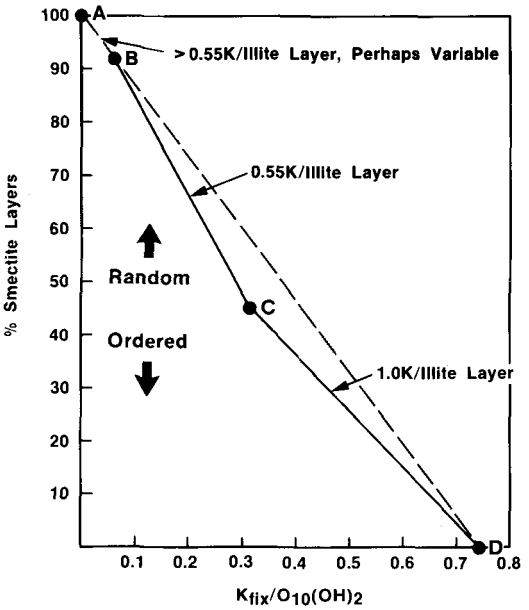

Figure 8. Plot of fixed potassium vs. expandability illustrating proposed interpretation of illitization process. See text.

A plot of CEC vs. expandability (Figure 4) for the Silurian set of samples is consistent with Figure 3. The relationship is linear and extrapolates to 15.3 meq/100 g for pure illite and 106 meq/100 g for pure smectite. A similar plot of surface area vs. expandability (Figure 5) for the Silurian samples shows a linear relationship that extrapolates to 154 m^2/g for pure illite and 812 m^2/g for pure smectite.

Because of the problems of interlaboratory accuracy mentioned previously, charge density vs. expandability is plotted separately for sets of samples analyzed by different techniques (Figure 6). Data for the Cretaceous samples from Montana are included for comparison, although they are probably inaccurate due to NaCl contamination. Recalculation by the method of Eslinger *et al.* (1979) corrected most of this error and gave octahedral occupancies reasonably close to 2.0. The data of Inoue and Utada (1983) also are shown in Figure 6. The plots show a characteristic break at about 50% smectite layers: Total charge density increases slightly with percentage of illite layers for the R=0 clays (smectite layers >50%), and much more sharply for the ordered clays (smectite layers <50%).

Plots of tetrahedral and octahedral charge vs. expandability show considerable scatter; large differences were observed for absolute values for different data sets (Figure 7). The common features are a stable octahedral charge with changing expandability and an increase in tetrahedral charge with increasing percentage of illite layers.

INTERPRETATIONS AND CONCLUSIONS

The accuracy of our measurements, as well as the fact that the same features were observed in four different sets of I/S samples, strongly suggests that the features described above are real. Furthermore, the statistical analyses also suggest that the data (Figure 2D) are fitted better by two lines rather than by a single line, with one line representing R=0 clays, and the other representing R>0 clays.

The shape of the curves (Figure 2) suggests that the amount of K per illite layer is not constant throughout the I/S series. This observation has already been made for glauconitic I/S by Thompson and Hower (1975, Table 6) and by Weaver and Pollard (1973, Figure 18). The extrapolated value of 0.75 fixed-K for pure illite thus represents an average for illite crystals, instead of the actual number of K atoms per illite layer. If 0.75 were the actual amount of fixed-K per layer, then the plot would be a straight line passing through zero fixed-K at 100% smectite, and through 0.75 K at 0% smectite.

The curve may consist of three segments: A–B, B–C, and C–D (Figure 8). The existence of segment A–B is speculative, and is based on wetting and drying experiments discussed below. The slope of segment B–C ($\Delta K/\Delta\%I$) shows that illite layers in this expandability interval have a relatively low charge density, containing about 0.55 K per layer. The slope of segment C–D indicates about 1.0 K per layer. Thus, an increasing proportion of the high-charge layers results in a gradual increase in the average fixed-K per layer. The curve extrapolates for pure illite to a value close to their arithmetic average because low- and high-K layers are almost equally abundant.

A tentative explanation for the possible existence of 3 types of illite layers in illite is as follows: The A–B segment of the curve, if distinct from the B–C segment, results from high-charge layers present in the original

https://doi.org/10.1346/CCMN.1986.0340403 Published online by Cambridge University Press

smectite. These first illite layers probably formed during a pre-diagenetic stage by collapse of the original high-charge smectite layers in the presence of K. Experimental evidence shows that high-charge smectite (for example, Otay montmorillonite) mixed with K-feldspar and subjected to wetting and drying cycles can strip K from the feldspar and fix it irreversibly, thereby producing as many as 30% illite layers (Środoń and Eberl, 1984a, 1984b). Low-charge smectites (e.g., Wyoming montmorillonite), contain only a few smectite layers with charge densities high enough to form illite layers by the aforementioned mechanism. The quantity of K per layer could vary in the A–B segment of the curve, indicating that segment A–B is not linear. If this interpretation is correct, the length of segment A–B in a given sequence of I/S should record the charge density of the original smectite.

The B–C segment of the curve represents formation of R=0 I/S by chemical transformation from smectite (e.g., Al for Si substitution). A charge of −0.55 is required to dehydrate interlayer K and fix it between adjacent 2:1 layers. Infrared data for the Carboniferous samples (Środón, 1980) show that this small value for fixed-K is not due to the presence of fixed ammonium ion, an ion that can proxy for K (Cooper and Abedin, 1981). Once about 50% of the layers have collapsed, the clay (ideally) is composed only of 20-Å thick illite layers. To decrease expandability further, it is necessary to join these 20-Å illite units together, thereby forming 40-Å thick particles. A charge of −1.0 is required for this dehydration due to polarization effects caused by adjacent illite layers (Sawhney, 1967), thereby giving rise to the C–D segment of the curve. The continuation of such a process results in the formation of illite crystals that contain alternating low- and high-K interlayers. Preservation of early-formed illite layers in illite suggests that the reaction proceeds by transformation rather than by neoformation, as does a stability for octahedral charge found throughout the mixed-layer series.

The I/S data can be extrapolated to characterize the illite end-member of the series. Illite formed from smectite in bentonites has an average apparent fixed-K content of ~0.75 per layer, and an average of 0.04–0.05 equivalents of exchangeable cations per layer attributable to external (edge) exchange sites, both summing to about −0.8 per $O_{10}(OH)_2$ total charge density. Such an illite has a CEC of 15 meq/100 g and a surface area of ~150 m^2/g. Smectite-derived illite consists mainly of two kinds of equally abundant layers containing ~0.55 and 1.0 K per $O_{10}(OH)_2$. In addition, a small amount of pre-diagenetic illite layers containing a variable quantity of K may be present. Illites formed by mechanisms other than the illitization of smectite in bentonite (for example, the illitization of kaolinite and feldspar, the neoformation of illite in sandstone pores, or the formation of illite in shales) may have chemistries different than those described here.

ACKNOWLEDGMENTS

J. Ś. acknowledges support from the U.S. Geological Survey, which allowed him to participate in this study. D.J.M. publishes by permission of the Director, British Geological Survey (NERC). Final preparation of this manuscript was aided by the Research Staff of the Cities Service Oil and Gas Corporation. We thank L. G. Schultz and G. Whitney for reviews of the initial manuscript.

REFERENCES

Carter, D. L., Heilman, M. D., and Gonzalez, C. L. (1965) Ethylene glycol monoethyl ether for determining surface area of silicate minerals: *Soil Sci.* **100,** 356–360.

Cooper, J. E. and Abedin, K. Z. (1981) The relationship between fixed ammonium-nitrogen and potassium in clays from a deep well on the Texas Gulf Coast: *Texas J. Sci.* **34,** 103–111.

Eslinger, E., Highsmith, P., Albers, D., and deMayo, B. (1979) Role of iron reduction in the conversion of smectite to illite in bentonites in the disturbed belt, Montana: *Clays & Clay Minerals* **27,** 327–338.

Grim, R. E., Bray, R. H., and Bradley, W. F. (1937) The mica in argillaceous sediments: *Amer. Mineral.* **22,** 813–829.

Hoffman, J. and Hower, J. (1979) Clay mineral assemblages as low grade metamorphic geothermometers—application to the thrust faulted disturbed belt of Montana, USA: *Soc. Econ. Paleontol. Mineral. Spec. Publ.* **26,** 55–79.

Hower, J. and Mowatt, T. C. (1966) The mineralogy of illites and mixed-layer illite/montmorillonites: *Amer. Mineral.* **51,** 825–854.

Hower, J., Schmittroth, L. A., Perry, E. C., and Mowatt, T. C. (1964) X-ray spectrographic major constituent analysis of undiluted silicate rocks and minerals: *Geol. Soc. America Program 1964 Ann. Meeting, Miami, Florida,* 96–97 (abstract).

Inoue, A. and Utada, M. (1983) Further investigations of a conversion series of dioctahedral mica/smectites in the Shinzan hydrothermal alteration area, northeast Japan: *Clays & Clay Minerals* **31,** 401–412.

Mackenzie, R. C. (1951) A micromethod for determination of cation-exchange capacity of clay: *J. Colloid Sci.* **6,** 219–222.

Medlin, J. H., Suhr, N. N., and Bodkin, J. B. (1969) Atomic absorption analysis of silicates employing $LiBO_3$ fusion: *At. Absorpt. Newsletter* **8,** 25–29.

Parachoniak, W. and Środoń, J. (1973) The formation of kaolinite, montmorillonite, and mixed-layer montmorillonite-illites during the alteration of Carboniferous tuff (the Upper Silesian Coal Basin): *Mineral. Polonica* **4,** 37–56.

Sawhney, B. L. (1967) Interstratification in vermiculite: in *Clays and Clay Minerals, Proc. 15th Natl. Conf., Pittsburgh, Pennsylvania, 1966,* S. W. Bailey, ed., Pergamon Press, New York, 75–84.

Środoń, J. (1976) Mixed-layer smectite/illites in the bentonites and tonsteins of the Upper Silesian Coal Basin: *Prace Mineral.* **49,** 1–84.

Środoń, J. (1980) Precise identification of illite/smectite interstratifications by X-ray powder diffraction: *Clays & Clay Minerals* **28,** 401–411.

Środoń, J. (1984) X-ray powder diffraction identification of illitic materials: *Clays & Clay Minerals* **32,** 337–349.

Środoń, J. and Eberl, D. D. (1984a) Illite: in *Micas,* S. W. Bailey, ed., Reviews in Mineralogy **13,** Mineralogical Society of America, Washington, D.C., 495–544.

Środoń, J. and Eberl, D. D. (1984b) Pre-burial and post-burial illitization of smectite: *Program with Abstracts, 21st Annual Meeting Clay Minerals Society,* Baton Rouge, Louisiana, p. 111.

Thompson, G. R. and Hower, J. (1975) The mineralogy of glauconite: *Clays & Clay Minerals* **23,** 289–300.

Weaver, C. E. (1965) Potassium content of illite: *Science* **147,** 603–605.

Weaver, C. E. and Pollard, L. D. (1963) *The Chemistry of Clay Minerals:* Elsevier, Amsterdam, 250 pp.

(Received 6 July 1984; accepted 25 September 1985; Ms. 1394)